Mausam, (1985), **36**, 2, 135-142

551.511.32

Use of 10-level balance model for diagnostic studies of vertical motion in tropics

A. V. R. K. RAO, L. K. MURTY, A. K. BOHRA and R. K. DATTA

India Meterological Department, New Delhi

(*Received 8 June 1983*)

सार — एक मानसून अवदाब के मामले में उर्ध्वाधर वेगों की एक 10-स्तर संतुलन मॉडल के द्वारा गणना करने का प्रयास वर्तमान अध्ययन में किया गया है। 10^{-3} मि०बार/से०के स्तर का अधिकतम उर्ध्वाधर वेग प्राप्त हुआ है। मानसून अवदाब में वर्षा बंटन का एक विशेष लक्षण, यह है कि दक्षिण-पश्चिमी क्षेत्र में व्यापक रूप से वर्षा होती है। यह मॉडल इसी क्षेत्र में अधिकतम उर्ध्वगामी गति दर्शाता है।

इसके परिणामों की तुलना भूविक्षेपी कल्प मॉडल तथा शुद्ध गतिक विधि द्वारा अभिकलित परिणामों से की गई है। कटिबन्धों में सन्तुलन मॉडल की अनुकूलता पर भी चर्चा हुई है।

ABSTRACT. In the present study an attempt has been made to compute vertical velocities by a 10-level balanced model in the case of a monsoon depression. Maximum vertical motion of the order of 10^{-3} mb/sec is obtained. A characteristic feature of the rainfall distribution in a monsoon depression is the occurrence of fairly widespread rainfall in the SW sector. This model depicts a maximum upward motion in the same sector.

The results have been compared with the computations made by quasi-geostrophic model as well as kinematic method. The suitability of the balance model in the tropics, has been discussed.

1. Introduction

To derive vertical motion field generally two techniques have been used; namely kinematic method and by the solution of well known Omega equation.

In India, the first attempt to compute vertical motion field was made by Das (1962) who computed vertical motion field for mean monsoon flow by solving the quasi-geostrophic Omega equation. Saha (1968) used kinematic method to compute vertical motion field for monsoon period. A number of other workers in India have used quasi-geostrophic Omega equation, with certain variations in physical processes, to compute vertical motion associated with various tropical disturbances (Rao and Rajamani 1968, Das *et al.* 1970, Mukherjee and Datta 1973, Sinha 1973, Ramanathan and Bansal 1975).

In the quasi-geostrophic formulation, there are inherent limitations of its application in the latitudes near the equator. Attempts have, therefore, been made to develop an Omega equation based on primitive equations. One such model called a balanced model was used by Krishnamurti and Baumhefner (1966). Subsequently Krishnamurti (1968), Baumhefner (1968), Sinha and Sharma (1981) used the same multi-level balanced model. Miller (1969) computed vertical velocities by a similar model with a slight variation in the formulation.

In this paper, we have used the model following Miller (1969) to compute vertical motion field in the case of two monsoon depressions. The vertical motion field pertaining to the depression of 1 August 1969 is presented in detail in this paper. The results have also been compared with the vertical motion field obtained by (*i*) kinematic method and (*ii*) quasi-geostrophic method (QGM) (Das *et al.* 1970).

2. Model description

2.1. *Basic-equations*

The horizontal equations of motion in x, y, p system are (meaning of symbols in Table 1)

$$\frac{\partial u}{\partial t} = -u\frac{\partial u}{\partial x} - v\frac{\partial u}{\partial y} - \omega\frac{\partial u}{\partial p} + fv - \frac{\partial \phi}{\partial x} + K_H \nabla^2 u + g\frac{\partial \tau_x}{\partial p} \quad (1)$$

$$\frac{\partial v}{\partial t} = -u\frac{\partial v}{\partial x} - v\frac{\partial v}{\partial y} - \omega\frac{\partial v}{\partial p} - fu - \frac{\partial \phi}{\partial y} + K_H \nabla^2 v + g\frac{\partial \tau_y}{\partial p} \quad (2)$$

The continuity equation may be written in the form

$$\nabla \mathbf{V} = -\partial\omega/\partial p \quad (3)$$

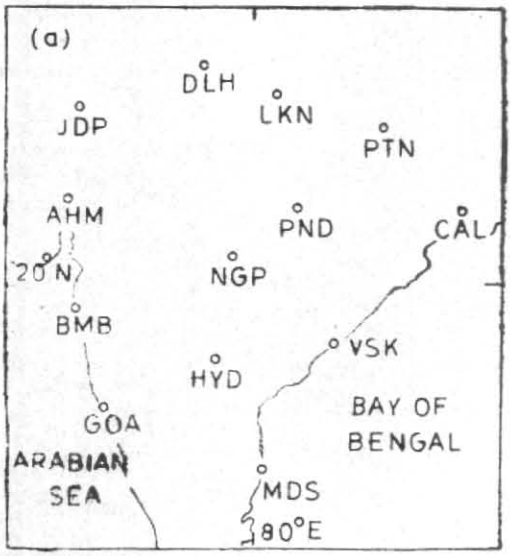

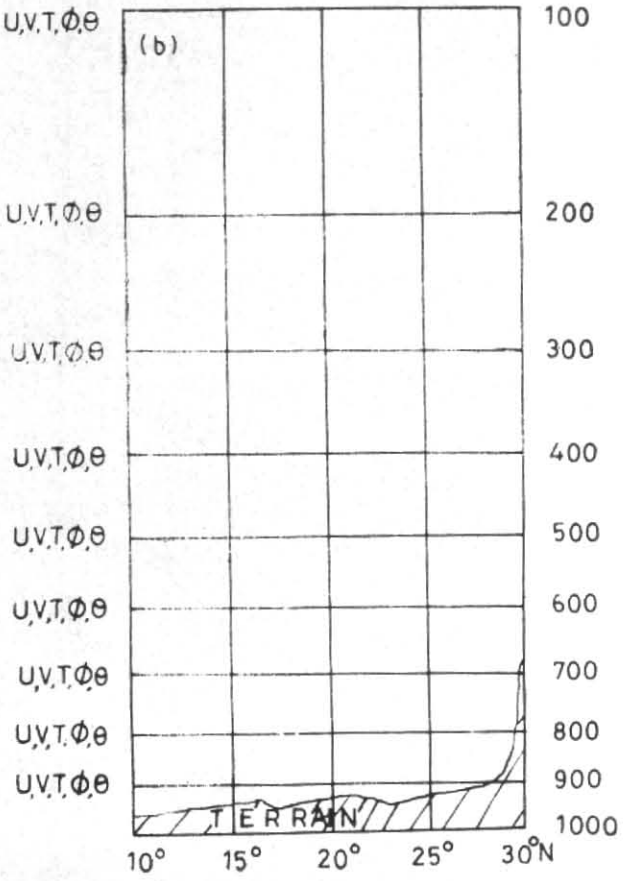

Figs. 1 (a&b). The Horizontal and vertical grids. Short lines on the boundaries indicate the grid points

The first law of thermodynamic equation is expressed by the equation

$$c_p T/\theta \left[\frac{\partial \theta}{\partial t} + \mathbf{V}. \nabla \theta + \omega \frac{\partial \theta}{\partial p} \right] = H \qquad (4)$$

where H is the rate of diabatic heating per unit mass of air. The hydrostatic equation is written as :

$$\frac{\partial \phi}{\partial p} = -\frac{RT}{p} \qquad (5)$$

and Poisson's equation as :

$$\theta = T\,(1000/p)^{R/c_p} \qquad (6)$$

The quantity π is written for

$$\pi = \frac{RT}{p\theta} \qquad (7)$$

and the static stability parameter is written as :

$$\sigma = -\frac{\alpha}{\theta} \frac{\partial \theta}{\partial p} \qquad (8)$$

The shearing stresses τ_x & τ_y are defined at 1000 mb in terms of the total wind speed, V_0 and a drag coefficient C_d

$$\tau_{x,\,o} = -\rho C_d V_o u \qquad (9)$$

$$\tau_{y,\,o} = -\rho C_d V_o v \qquad (10)$$

At the upper level, these quantities are defined by use of eddy viscosity for vertical mixing K_p

$$\tau_x = -\frac{K_p}{g} \frac{\partial u}{\partial p} \qquad (11)$$

$$\tau_y = -\frac{K_p}{g} \frac{\partial v}{\partial p} \qquad (12)$$

where, K_p is in the (x, y, p) system and is related to K_M in the x, y, z system as $K_p = \rho^2 g^2 K_M$. A constant value of 5×10^{-3} is assumed for C_d. The value of K_H, a lateral mixing coefficient is taken as 3×10^8 cm^2 sec^{-1} (Barrientos 1964). The value of K_p is used as given by Krishnamurti (1973).

By differentiating Eqn. (1) w.r.t. y and Eqn. (2) w.r.t. x and subtracting the former from the later, we obtain the vorticity equation. Similarly divergence equation is obtained by diffentiating (1) w.r.t. x and (2) w.r.t. y and by adding both. The Omega Eqn. (13) is obtained by operating by $\partial^2/\partial t \partial p$ on the divergence equation and substituting for (*i*) term $\partial \zeta/\partial t$ from the vorticity equation, (*ii*) terms $\partial^2 \phi/\partial t \partial p$ from the hydrostatic Eqn. (5) and (*iii*) term $\partial \theta/\partial t$ from the thermodynamic energy Eqn. (4).

$$\nabla^2(\sigma\omega) + f\eta \frac{\partial^2 \omega}{\partial p^2} - f\omega \frac{\partial^2 \eta}{\partial p^2}$$

$$-f \frac{\partial}{\partial p} \left(\frac{\partial \omega}{\partial x} \frac{\partial v}{\partial p} - \frac{\partial \omega}{\partial y} \frac{\partial u}{\partial p} \right) =$$

$$= -f \frac{\partial}{\partial p} (\mathbf{V}. \nabla \eta) - fK_H \nabla^2 \frac{\partial \eta}{\partial p} - fg \frac{\partial^2}{\partial p^2} \left(\frac{\partial \tau_y}{\partial x} - \frac{\partial \tau_x}{\partial y} \right) +$$

$$+\pi\nabla^2(\mathbf{V}.\nabla\theta)-\nabla^2\left[\frac{R}{p}\frac{\partial}{\partial p}(K_p\,\partial\theta/\partial p)\right]$$

$$-\nabla^2\frac{R}{p}\left(K_H\nabla^2\theta\right)-\nabla^2\frac{R}{p}(H/c_p)+$$

$$+\pi\nabla^2\,\partial\theta/\partial t+f\frac{\partial}{\partial t}\left(\partial\eta/\partial p\right) \qquad (13)$$

As this is a diagnostic study, the time dependent terms are not considered in calculation. The heating term is also not evaluated. The following are the various terms of the forcing function :

(1) $f\frac{\partial}{\partial p}\left(\mathbf{V}.\nabla\eta\right)$

Differential absolute vorticity advection

(2) $\pi\nabla^2(\mathbf{V}.\nabla\theta)$

Laplacian of thermal advection

(3) $-f K_H\nabla^2(\partial\eta/\partial p)$

Horizontal diffusion of vertical absolute vorticity gradient

(4) $-fg\partial^2/\partial p^2\left(\frac{\partial\tau_y}{\partial x}-\frac{\partial\tau_x}{\partial y}\right)$

Effect of frictional stresses

(5) $-\nabla^2\left[\left(\frac{R}{p}\right)\frac{\partial}{\partial p}\left(K_p\frac{\partial\theta}{\partial p}\right)\right]$

Laplacian of differential advection of stability

(6) $-\nabla^2 R/p\,(K_H\nabla^2\theta)$

Laplacian of horizontal thermal diffusion

(7) $-\nabla^2 R/p\,(H/c_p)$

This consists of the combined effects of latent heat (H_L) and sensible heat (H_S) transfer from the water surface to the atmosphere ($H=H_S+H_L$).

(8) $\pi\nabla^2\partial\theta/\partial t$

Laplacian of local temperature changes.

(9) $f\frac{\partial}{\partial t}\left(\partial\eta/\partial p\right)$

Local change of vertical absolute vorticity gradient

Neglecting the time derivative terms, the Omega equation for dry model becomes :

$$\nabla^2(\sigma\omega)+f\eta\partial^2\omega/\partial p^2-f\omega\partial^2\eta/\partial p^2-f\frac{\partial}{\partial p}\left(\frac{\partial\omega}{\partial x}\frac{\partial v}{\partial p}\right.$$

$$\left.-\frac{\partial\omega}{\partial y}\frac{\partial u}{\partial p}\right)=f\frac{\partial}{\partial p}(\mathbf{V}.\nabla\eta)-fK_H\nabla^2\partial\eta/\partial p$$

$$-fg\frac{\partial^2}{\partial p^2}\left(\frac{\partial\tau_y}{\partial x}-\frac{\partial\tau_x}{\partial y}\right)+\pi\nabla^2(\mathbf{V}.\nabla\theta)$$

$$-\nabla^2 R/p\,(K_p\,\partial\theta/\partial p)-\nabla^2K_H\nabla^2\theta \qquad (14)$$

Thus the forcing function of the above balance equation contains 6 terms while the forcing function in the quasi-geostrophic model contain only the 1st and 4th terms. Though the contribution of the remaining terms is comparatively smaller, nevertheless, their inclusion in the equation gives a better insight about the processes responsible for the resultant vertical motion which is not obtainable from a quasi-geostrophic model.

The present model consists of 10 levels starting from surface to 100 mb at an interval of 100 mb. In the horizontal, the resolution is 2° Lat./Long. for the area extending from 10 N to 30 N and 70 E to 90 E. The grids are shown in Figs. 1 (a & b).

We used this 10-level balanced model for diagnostic calculation of vertical motion field in the case of two depressions. However, in this paper, the study of depressions of 1 August 1969 is presented as the results of the study by Q. G. model are available for comparison (Das *et al.* 1970).

2.2. *Boundary conditions for* ω

The two boundary conditions are $\omega=0$ at the top level, *i.e.*, 100 mb and the ω is calculated at the lower boundary by using Cressman's formula :

$$\omega_{LB}=\mathbf{V}.\nabla p_s+\rho g/f\left[\frac{\partial}{\partial y}C_D u V_0-\frac{\partial}{\partial x}C_D v V_0\right] \qquad (15)$$

Inclusion of orography : The terrain is also included by calculating the lower boundary vertical velocity at the top of the hills by using the above formula and below that level ω is taken as zero. This means, at the points within the grid, where ω is zero (within the terrain) forcing is not calculated during relaxation. The smoothed terrain heights as given by Berkofsky and Bertoni (1960) are used with the exception that the highest terrain is limited to equivalent of 600 mb.

3. Case study

3.1. *Synoptic situation*

A depression formed over the north Bay of Bengal on 28 July 1969 and lay centred near about 100 km north of Pendra at 0300 GMT on 1 August 1969. The associated cyclonic circulation extended upto 7.2 km above sea level. It weakened into a low pressure area over southeast Uttar Pradesh and adjoining northwest Madhya Pradesh on 2nd morning. The surface pattern is presented in Fig. 2.

3.2. *Generation of data set*

The quasi-geostrophic models need only one parameter, namely the geopotential height, as input. The balance models, as can be seen from the model description in the section 2.2, requires u, v, ϕ and T at various levels as input. This makes the problem more difficult, since these parameters must be mutually consistent and

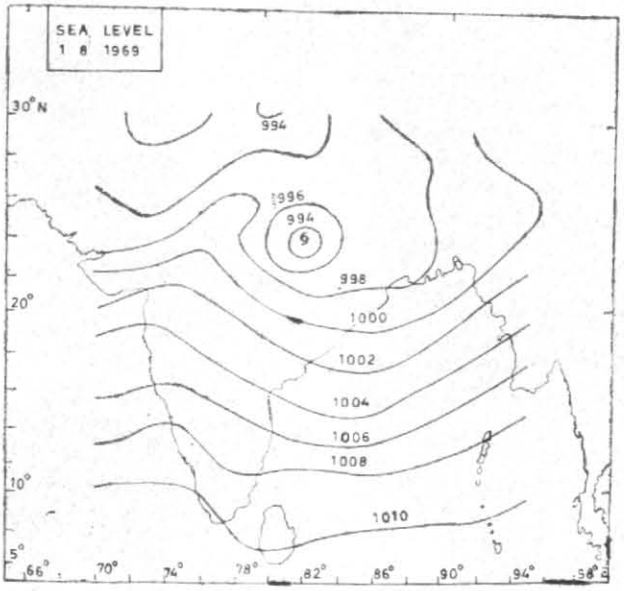

Fig. 2. Sea level pattern at 03 GMT of 1 August 1969

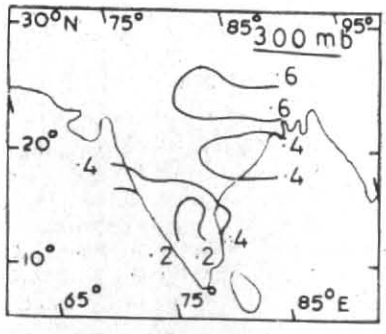

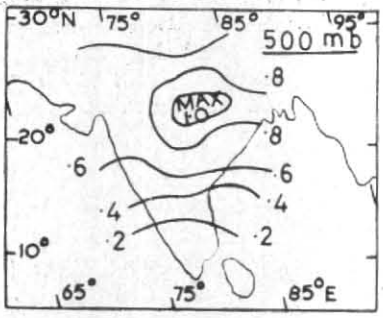

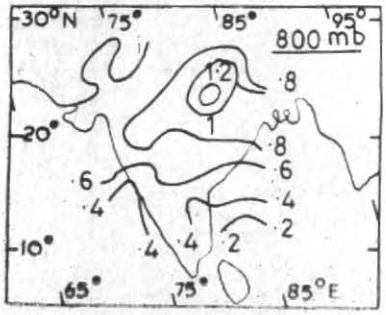

Fig. 3(a). Absolute vorticity pattern at 800, 500 & 300 mb (Unit : 10^{-4} sec^{-1})

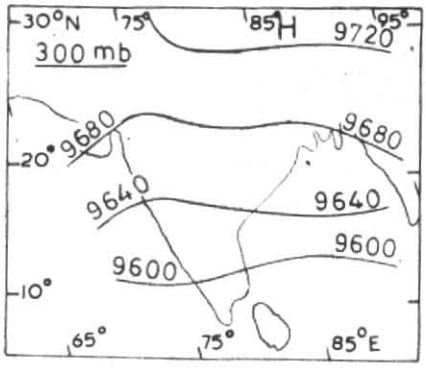

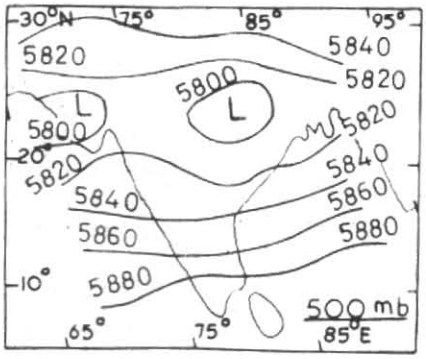

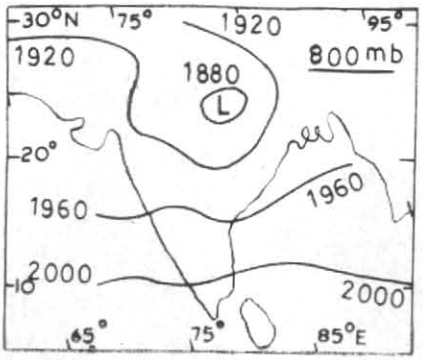

Fig. 3 (b). Geopotential field at 800, 500 and 300 mb in gpm

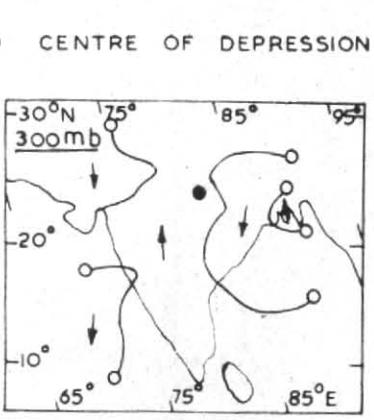

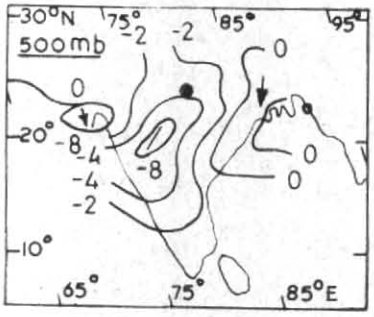

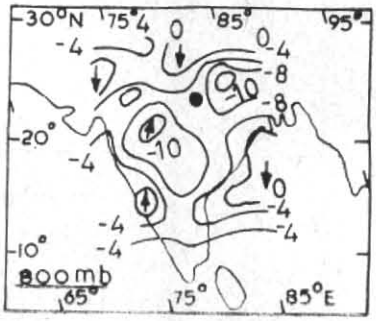

Fig. 4. Vertical velocity pattern at 800, 500 & 300 mb (Unit : 10^{-4} mb sec^{-1})

TABLE 1

Meaning of the symbols used in the equations

Symbol	Meaning	Units and order of magnitude
Cd	Drag coefficient	5×10^{-3}
c_p	Specific heat of air at constant pressure	240 cal/gm/°K
f	Coriolis parameter	10^{-4} sec^{-1}
f_0	Mean value of Coriolis parameter	10^{-4} sec^{-1}
g	Acceleration due to gravity	980 cm sec^{-2}
H	Total heating function	cal/gm/sec
K_H	A coefficient for Lateral mixing	10^8 cm^2/sec
Kp	A coefficient for vertical mixing	10^4 dynes^2/sec dynes/cm^2
p	Pressure	
R	Gas constant	2.86×10^6 erg/gm/°K
t	Time	sec
T	Temperature	°K
T^*	Virtual temperature	°K
u	Zonal component of the wind	cm sec^{-1}
v	Meridional component of the wind	cm sec^{-1}
V	Horizontal velocity vector	cm sec^{-1}
X	Distance in E-W direction	2×10^7 cm
Y	Distance in N-S direction	$2 \cdot 10^7$ cm
a	Specific volume	10^3 cm^3 gm^{-1}
β	$\partial f/\partial y$	10^{-13} sec^{-1} cm^{-1}
ζ	Relative vorticity	sec^{-1}
η	Absolute vorticity	sec^{-1}
θ	Potential temperature	°K
π	$RT/p\theta$	1 gm^{-1} cm^3 °K^{-1}
ρ	Density	1×10^{-3} gm cm^{-3}
ϕ	Geopotential	10^8 cm^2 sec^{-2}
σ	Static stability	10^{-3} to 10^{-2} cm^4 gm^{-2} sec^2
τx, τy	Horizontal shearing stresses	10^{-1} gm cm^3 sec^{-2}
ω	dp/dt vertical p velocity	10^{-4} mb sec^{-1}
∇^2	Horizontal Laplacian operator	10^{-14} cm^{-2}
J	Jacobian operator	10^{-14} cm^{-2}

also consistent with the model. A detailed scheme similar to the one proposed by Miller (1969) was used to generate the data for the model. The procedure is briefly described below :

3.2.1. *Generation of wind field*

Wind field is analysed over a larger area comprising whole of India, Pakistan and Burma. Charts are analysed starting from surface to 100 mb at an interval of 100 mb. Wind analysis is performed by drawing streamlines and isotachs. Geopotential field is also analysed to pick up the east-west and north-south boundary values to be used in the balance equation. Radiosonde data is augmented with the pilot balloon and aircraft observations. Below 500 mb, over Himalayan region, the data is fictitiously fitted to maintain continuity with the surroundings. From these analysed charts, grid point data is subjectively interpolated at 2° Lat./Long. grid points. This forms the data set for the model.

The u and v components of the wind were smoothed once in the horizontal by using a 9-point smoothing operator and a coefficient of 0.50 (Shuman 1957 b), and once in the vertical over three points. Smoothing in vertical is restricted upto 300 mb level only.

For computation of all derived parameters, *viz., vorticity and geopotential field, this smoothed wind* field is used.

3.2.2. *Generation of geopotential field*

It is well known that measurements of geopotential and temperature are less reliable over tropical regions, than the wind field. It is, therefore, necessary to derive the height field from the wind field. This was achieved by the use of balance equation at all the levels :

$$\nabla^2\phi = f\zeta - \beta u + 2\mathbf{J}(u, v)$$

The height values in gpm, at the boundary points are given from the analysed charts. The relaxation is carried out for the solution of ϕ, with the relaxation coefficient of 1.40 and to the accuracy of 1 metre.

3.2.3. *Generation of temperature field*

The temperature field is obtained from the height field by using the formula :

$$\frac{\partial\phi}{\partial p} = -\frac{RT}{p}$$

The temperature thus obtained is taken as the temperature representing the middle point of the layer. The temperature at 1000 mb is calculated subject to the condition that at 1000 mb the temperature should differ from the mean virtual temperature for the 1000 mb to 850 mb layer by a constant value based on climatology. Potential temperatures are calculated using Poisson's equation. The potential temperature at 100 mb is calculated from the temperature of 200 mb and using a lapse rate of 8°C/km (climatological value) between 200 and 100 mb and contour heights of the two levels.

By this procedure temperature, wind and height fields which are consistent with each other can be obtained to be used as input for the model.

4. Solution of Omega equation

The 'ω' Eqn. (13) is an elliptical equation and is solved by a standard Liebmann method of over-relaxation. The finite difference formulation is similar to the one used for the solution of quasi-geostrophic 'ω' equation. For the solution to be converging, the condition of ellipticity has to be satisfied. It tends to deviate from the elliptic condition when the static stability parameter becomes negative or the absolute vorticity becomes negative. It happens at isolated points. The programme provide the facility to check these conditions and whenever these occur, the value of static stability parameter or the absolute vorticity is replaced by an average of the neighbouring four points in y-axis. This procedure has been found to ensure convergence of the solution. Normally it was possible to get converged solution correct to 10^{-9} mb sec^{-1} in about 50 iterations.

5. Discussion of the results

5.1. *Vorticity field*

In Fig. 3 (a), we present the fields of absolute vorticity at 800 500 and 300 mb levels. Maximum absolute vorticity of the value 1.2×10^{-4}sec^{-1} is seen at the centre of the depression at 800 mb. There is no substantial change in its magnitude upto 500 mb. It reduced to half of its value at 300 mb. In an intense monsoon depression, various workers have observed the absolute vorticity of the value as high as 2.0×10^{-4} sec^{-1}. The value of absolute vorticity of 1.2×10^{-4}sec^{-1} of the present depression may well agree with the intensity of the depression which is in its weakening stage.

5.2. *Geopotential field*

Fig. 3(b) depicts the balanced geopotential field at 800, 500 and 300 mb levels. A low is seen at 800 and 500 mb. The circulation is extending upto 7.2 km and a trough aloft.

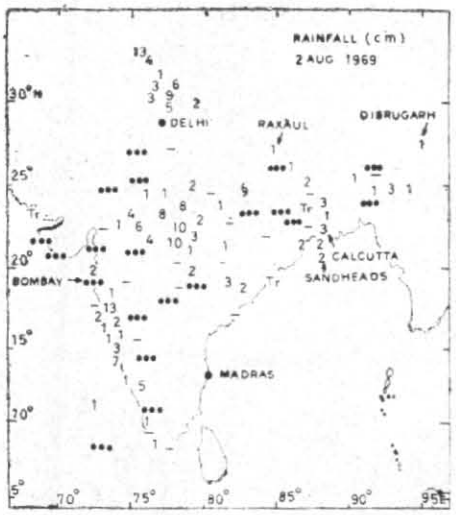

Fig. 5. Rainfall chart of 03 GMT on 2 August 1969

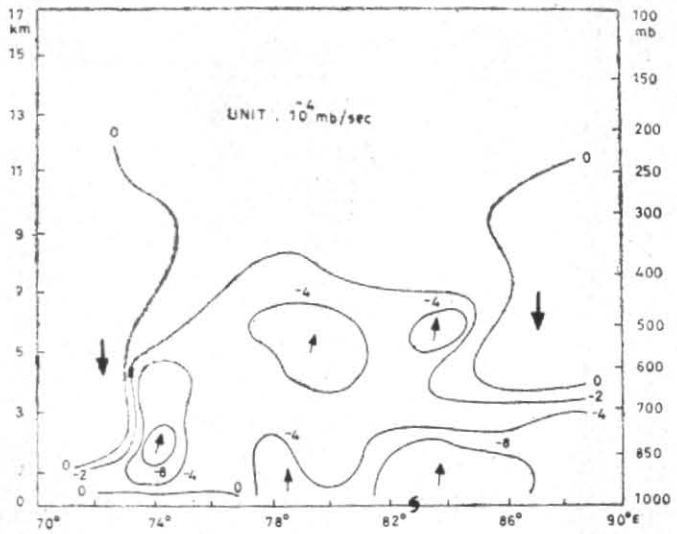

Fig. 6. Zonal cross-section of vertical motion field along 24N

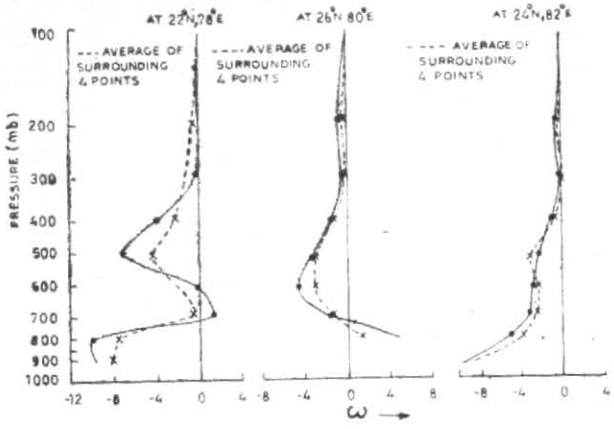

Fig.7. Vertical variation of ω at three selected points in SW sector, near the centre and NW sector

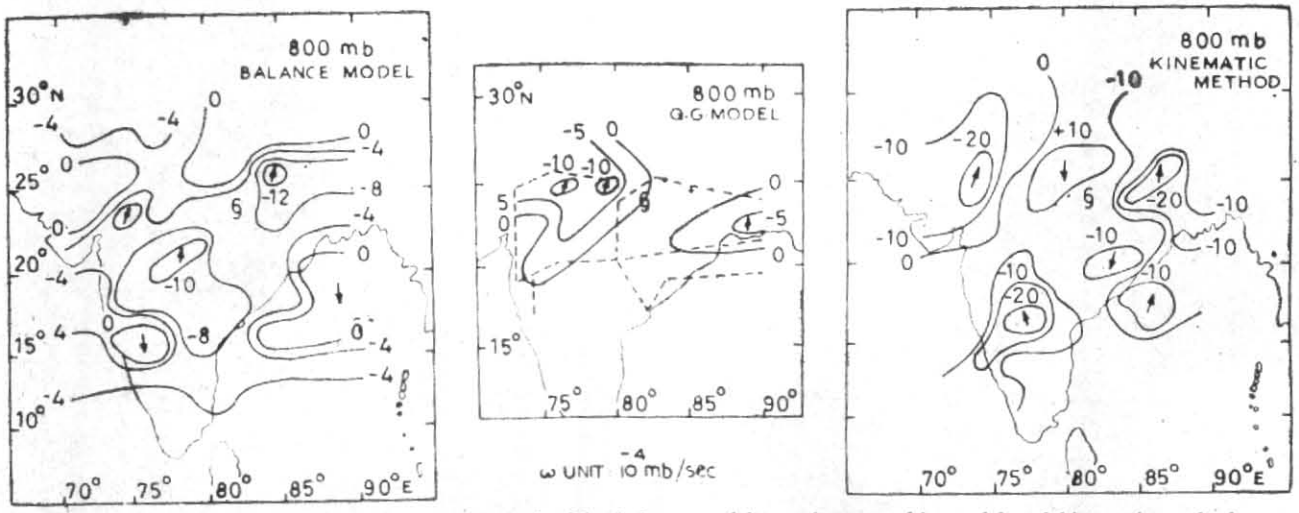

Fig. 8. Comparison of vertical motion field obtained by balance model, quasi-geostrophic model and kinematic method

TABLE 2

Contributions to the vertical motion by each of the terms of the forcing functions at different points in the four sectors of the depression in the lower & upper troposphere (Units : 10^{-5} mb/sec)

Term	SW sector (22N, 78E)	NE sector (26N, 84E)	Centre (24N, 82E)	NW sector (26N, 78E)	SE sector (22N, 86E)	SW sector (22N, 78E)	NE sector (26N, 84E)	Centre (24N, 82E)	NW sector (26N, 78E)	SE sector (22N, 86E)
	800 mb					300 mb				
$f\,\partial/\partial p\,(\mathbf{V}.\nabla\eta)$	—3.6	7.4	2.8	6.3	2.1	—7.3	—2.2	—5.6	2.4	—7.8
$\pi\,\triangle^2\,(\mathbf{V}.\nabla\theta)$	—9.7	—40.7	—7.1	—5.8	17.9	0.5	3.4	2.9	0.7	8.7
$-f\,K_H\,\nabla^2\,(\partial\eta/\partial t)$	—0.3	—0.4	—0.4	—0.2	0.3	—0.7	—0.3	—0.4	—0.3	—0.4
$-f\,g\,\frac{\partial^2}{\partial p^2}\,(\frac{\partial\tau_y}{\partial x}-\frac{\partial\tau_x}{\partial y})$	—0.5	—0.1	—0.1	—0.2	—0.1	1.1	0.4	0.5	0.7	0.7
$-\nabla^2\,[R/p\,(\frac{\partial}{\partial p}\,K_p\,\partial\theta/\partial p)]$	0.5	0.6	0.98	0.1	1.2	1.6	0.4	0.6	1.1	0.8
$-\nabla^2(\,R/p\,K_H\,\nabla^2\,\theta\,)$	0.3	0.5	0.89	0.2	0.01	0.7	0.2	0.4	0.3	0.2
Total	—13.3	—32.3	—2.9	0.4	21.4	—4.1	1.9	—1.6	4.9	2.2

5.2.1. *Contribution of the terms*

The Eqn. (14) used to evaluate the vertical motion field consists of 6 terms. In order to evaluate the contribution of each term, we calculated 'ω' field by considering one term at a time, as forcing, except the heating and the time derivative terms. The results of computation for 5-grid points near and around the centre of the depression are given in the Table 2 for two levels 800 mb and 300 mb, representing lower and upper troposphere respectively. It can be seen that the vorticity advection and the thermal advection terms are of the same order while the remaining terms are one order less than these two, both in the lower and upper troposphere. In the south of the depression centre, these two terms are in phase with each other while they are in the opposite direction in the north and near the centre of the depression, in the lower troposphere. Contribution from the thermal advection is more in the lower troposphere while the vorticity advection predominates in the upper troposphere. The dominant contribution from the thermal advection term in the lower troposphere suggests that the depression is baroclinic.

5.2.2. *ω-field and precipitation*

Fig. 4 presents the vertical motion field obtained for the case under study. The field at 800, 500 and 300 mb is presented. There are two centres of significant vertical motion, one in the SW sector and the other in the NE sector. The maximum vertical motion is -13×10^{-4}mb sec^{-1} at 800 mb level. Downward motion is observed in the NNW sector and a little away from the centre in the SE sector. The pattern at 500 mb also shows the axis of vertical motion is oriented in the SW and NE direction. At 300 mb, the field is weak upward motion near the centre surrounded by weak downward motion.

In Fig. 5, we have presented the rainfall distribution as recorded at 0300 GMT on 2 August 1969. In general, the areas of upward motion agree well with the area of precipitation. Point of special interest is that the region of maximum vertical motion in the SW sector of the depression (at 800 and 500 mb levels) is in close agreement with the area of the heavy rainfall which is typical of monsoon depressions. Even in the NE sector, where there is a second maximum of upward motion, the rainfall distribution is fairly widespread.

5.2.3. *Study of cross-section of ω-field*

The zonal vertical cross section along 24 N which runs close to the centre of the depression,is presented in Fig. 6. Upward motion is found in the central region with the downward motion both to the east and west of the system. Maximum vertical motion is located to the west of the centre. Another maximum is seen in the middle troposphere above the depression centre between 600 and 500 mb. Similar results were also obtained by Rao and Rajamani (1975). who used Q.G. model to compute vertical motion, and Sreerama Daggupaty & Sikka (1977).

5.2.4. To further examine the structure of the ω-field, we also prepared the vertical distribution of its field at 3-grid points pertaining to (1) near the centre of the depression, (2) over a point of upward motion (SW sector), (3) over a point of downward motion (NW sector). These are presented in Fig. 7. The ω-field at the point, and the average of surrounding grid points are compared and presented in the above figure. The full curve represents the values at the point and dotted curve represents the average of the surrounding 4 points. Both the curves show similar patterns. At the centre, the upward motion prevailed at all the levels with initial increase in the magnitude upto 500 mb level and gradually decreasing later. At the other two points, ω changed its sign near about 700 mb and reached a maximum positive or negative value at 500 mb. This indicates that there may be two levels of non-divergence one at about 700 mb and the other at about 500 mb (at the maximum and minimum of vertical motion).

Comparison of results with other studies

Das *et al.* (1970) presented the vertical velocity field for the same depression by a ten layer Q.G. model,

Vertical motion field at 800 mb of their calculations is presented in Fig. 8(b).

We also computed vertical motion for the same case by kinematic method by integrating the continuity Eqn. (3). The divergence is calculated by the formula :

$$\frac{\partial u}{\partial x} + \frac{\partial v}{\partial y} = \text{Div } \mathbf{V}$$

The divergence at each level is adjusted such that the net divergence in the vertical column is zero (O' Brien 1970). These values are used during the integration to compute the value of ω at each level using the following boundary condition for the lower level.

$$\omega_{LB} = \mathbf{V} . \nabla p_s$$

The results for 800 mb level are presented in Fig. 8(c). Comparison of the results with Das *et al.* (1970) and kinematic method with the present model shows that the vertical motion with the balance model agrees best with the rainfall pattern. The kinematic method gives higher values while the Q.G. model under estimates the vertical motion. Moreover, the maximum vertical motion in the Q.G. model is obtained not in the SW sector but in the west of the depression. The kinematic method shows downward motion near the centre of the depression, while the balance model and Q.G. model indicate upward motion. The input data for computation of vertical motion field in all the methods was subjectively analysed. The difference in performance to some extent may be related to the input data but, we believe largely the improvement in the performance is technique dependent.

More cases are being run on real time basis to study the use of balance model for operational purposes.

6. Summary

The following conclusions are drawn :

(*i*) The vertical motion pattern calculated by a diagnostic balanced model depicts better agreement with the rainfall distribution than with any other method. In the tropical regions this model suits better for diagnostic studies.

(*ii*) The level of non-divergence is located between 800 & 700 mb in the lower troposphere. In the lower levels, frictional forces play a significant part in the upward motion.

(*iii*) Though the Laplacian of thermal advection and differential vorticity advection are the dominating terms in deciding the vertical motion, the contributions from the other terms are also important. The predominance of thermal advection term in the lower troposphere suggests that the depression is maintained by baroclinic forces.

Acknowledgements

The authors wish to express their grateful thanks to Dr. R.P. Sarker, ADGM (S) for his valuable suggestions. They also express their sincere thanks to Dr. H. S. Bedi for useful discussions and for his suggestions during the course of this work. Thanks are also due to Shri G. S. Mandal for his suggestions after going through the manuscript. to Shri Manohar Lal for plotting the charts and Shri Verinder Kumar for typing the manuscript. They express their thanks to the colleagues in the Computer Unit for their help during the development of the programme. They wish to express their greatful thanks to the referee for his constructive suggestion.

References

Banner, I. Miller, 1969, 'Experiment in Forecasting Hurricane Development with Real Data ESSA,' Tech. Mem. No. 85.

Barrientos, C. S., 1964, 'Computations of transverse circulations in a steady state symmetric hurricane', *J. appl. Met.*, **3**, pp. 685-692.

Baumhefner, P. David, 1968, 'Application of a diagnostic numerical model to the tropical atmosphere', *Mon. Weath. Rev.*, **96**, 4, pp. 218-228.

Bellamy, John C., 1949, 'Objective calculations of divergence vertical velocity and vorticity', *Bull. Am. Met. Soc.*, **30**, 2, pp. 45-49.

Berkofsky, L. and Bertoni, E. A., 1960, 'Topographic charts at one degree intersections', AFCRL-TN-60-615 GRD Res. Notes No. 42.

Das, P. K., Datta, R. K. and Chhabra, B. M., 1970, 'Diagnostic study of vertical motion, *vis-a-vis* large scale cloud systems', India Met. Dep. Sci. Rep. No. 126.

Datta, R. K. and Mukherjee, T. K., 1975, 'Vertical velocity patterns over India and neighbourhood during break monsoon and active monsoon periods', *Indian J. Met. Hydrol. Geophys.*, **26**, pp. 399-404.

Krishnamurti, T. N. and Baumhefner, D., 1966, 'A structure of a tropical disturbance based on solution of a multilevel baroclinic model, *J. appl. Met.*, **5**, 4, pp. 396-406.

Krishnamurti, T. N., 1968, 'A diagnostic balance model for studies of weather, systems of low and high latitudes', *Mon. Weath. Rev.*, **96**, 4, pp. 197-207.

Krishnamurti, T. N., Masao, Kanamitsu, Ben Ceselski and Mathur, M. B., 1973, 'Florida State Univ. Tropical Prediction model', *Tellus*, **15**, pp. 524-535.

Mukherjee, T. K. and Datta, R. K., 1973, 'Prognosis by four layer quasi-geostrophic model', *Indian J. Met. Geophys.*, **24**, pp. 93-100.

O'Brien, J. J., 1970, 'Alternative solutions to the classical vertical velocity problem', *J. appl. Met.*, **9**, pp. 197-203.

Ramanathan, Y. and Bansal, R. K., 1976, 'The NHAC quasi-geostrophic model—Part I : The physical description of the model, India Met. Dep. Sci. Rep. 76/1.

Rao, K.V. and Rajamani, S., 1968, 'Diagnostic study of a monsoon depression by geostrophic baroclinic model', Institute of Tropical Met., Pune Sci. Rep. No. 54.

Rao, K. V. and Rajamani, S., 1975, *Indian J. Met. Hydroi. Geophys.*, **26**, pp. 369-374.

Saha, K. R., 1968, 'On the instantaneous distribution of vertical velocity in the monsoon field and structure of monsoon circulation', *Tellus*, **20**, pp. 601-619.

Shuman, F. G., 1957, 'Numerical methods in weather prediction I. The balance equation', *Mon. Weath. Rev.*, **85**, pp. 329-332.

Sinha, M. C., 1973, 'Computation of vertical velocities in the Indian region by quasi geostrophic diabatic Omega Equation of four level model', India Met. Dep. Sci. Rep. No. 194.

Sinha, M. C. and Sharma, O. P., 1981, 'Vertical motion in the monsoon circulation. Monsoon Dynamics, International Symp. on Monsoon Dynamics Delhi, 1977, pp. 601-613.

Sreerama, M. Daggupaty & Sikka, D. R., 1977, 'On the vorticity budget and vertical velocity distribution associated with the life cycle of a Monsoon Depression, *J. atmos. Sci.*, **34**, pp. 773-792.